AN ULTRA-COMPACT, HIGH-ACCURACY STAR TRACKER. P. H. Sorensen[1], B. J. Davis[2], R. J. Kline-Schoder[3], and R. L. Morrison[4]. [1]Creare LLC, 16 Great Hollow Road, Hanover, NH 03755; phs@creare.com. [2]Creare LLC, 16 Great Hollow Road, Hanover, NH 03755; bjd@creare.com. [3]Creare LLC, 16 Great Hollow Road, Hanover, NH 03755; rjk@creare.com. [4]Distant Focus Corporation, 1715 Ironhorse Drive, Suite 260, Longmont, CO, 80501; morrison@distantfocus.com.

Introduction: NASA has identified the need for the development of technology for smaller, more cost effective satellites that will enable it to continue to conduct vital space missions in the future despite limited resources. To realize this goal, NASA sees the need for beyond state-of-the-art research to drastically reduce the size, weight, and power (SWAP) of satellite payloads and satellite subsystems. One such subsystem is the attitude determination and control system (ADCS). Precision ADCSs require accurate, arc-second-level attitude determination sensors for three-axis stabilization, which are currently unavailable for small satellites. Current large satellite star trackers are too large, too costly, and too power hungry for use with small satellites. There is therefore a need to develop a new miniaturized star tracker that will provide high accuracy attitude measurements in a package that is small, uses little power, has low mass, and costs a fraction of current star trackers. Such trackers could also find use on sounding rockets, high-altitude science balloons, and missions to the outer planets that NASA is heavily involved in.

The Need for a Compact Star Tracker: For Earth and many planetary missions, critical-state parameter measurements of the atmosphere are vector quantities and thus require instruments to make vector measurements to properly quantify them. Instruments such as electric field probes, magnetometers, retarding potential analyzers (RPAs), and ion drift meters (IDMs) have been relied on for decades to provide vector measurements of electric and magnetic fields and information on the direction and magnitude of the motions of charged particles in the atmosphere.

These types of instruments all require accurate satellite pointing to orientate the vectors they measure. Some of these instruments, such as the RPAs, are "weakly" impacted by pointing error. A 5° pointing error results in a roughly 25 m/s ion drift velocity error as measured by an RPA. Drifts are usually on the order of hundreds of meters per second, implying that an RPA mounted on a typical satellite with no star tracker could expect velocity errors on the order of 10%. Other instruments, such as the IDM, are "strongly" impacted by pointing error. A 5° error in this case would result in an over 500 m/s error in the measured ion drift velocity. Such an error would be on the order of the quantity being measured and thus render a satellite-based IDM measurement useless. Most other vector instruments would fall somewhere between these two extremes. Some would be negatively impacted by large pointing errors but still useful, while others would become impractical altogether.

While many of the instruments themselves are currently being miniaturized and power optimized, many of them will not be viable on all satellites until tight attitude determination accuracy requirements have been met. Only then will low-cost satellites that can be built by a wide variety of institutions including universities, government agencies, and private companies begin to become a widespread tool in the space science community.

Ultra Compact Star Tracker: Creare developed an Ultra Compact Star Tracker (UST) design that is estimated to have a mass of less than 650 g, a volume of less than 400 cm^3, and consumes less than 0.5 W of power, while providing an estimated attitude accuracy of 1 arc second in pitch and yaw and 10 arc seconds in roll. Analysis of the design further shows that the UST will be able to withstand the radiation environment typical for a two- to five-year LEO mission and will also be able to track attitude changes, as well as determine attitude without prior orientation knowledge (i.e., perform "Lost in Space" operation).

Our UST combines a novel optical design with a high resolution, complementary metal oxide semiconductor (CMOS) imaging sensor, a highly efficient field-programmable gate array (FPGA) processor, and a star identification algorithm based on a star catalog for all stars brighter than apparent magnitude m=7. A central new feature of this star tracker is the use of a folded mirror optical system (Figure 1) that collects the light in an annular aperture and, through multiple reflections, focuses it on the imager. The advantages of this design over a standard refractive optics design are (1) a very compact design can be achieved without sacrificing accuracy; (2) the light-gathering aperture is much larger (given a fixed instrument mass and image quality), which leads to better sensitivity; (3) the aperture geometry makes the sun shielding baffles smaller and unobtrusive; and (4) the imaging sensor can be shielded efficiently from cosmic radiation, since it is not directly exposed to space.

Figure 2 captures some of the key technical specifications of the UST and how they compare to currently available star trackers.

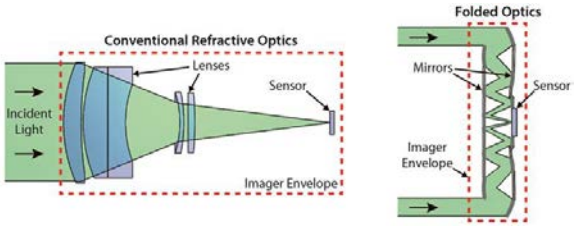

Figure 1: Standard refractive optics (left) require long focal lengths and bulky multi-element assemblies for high precision imaging. The equivalent folded optic (right) is less massive and occupies a smaller volume. The annular collection aperture also allows direct shielding of the sensor.

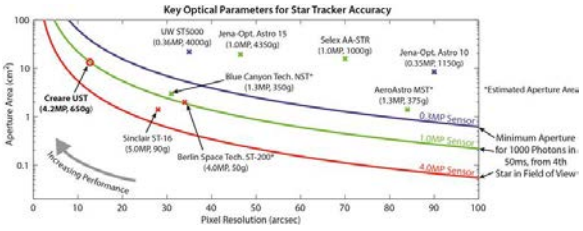

Figure 2: Comparison of Pixel Resolution (Affects Accuracy) and Aperture Area (Affects Sensitivity) for the Creare UST and Existing Star Trackers. The Creare UST provides an unprecedented combination of large aperture size, fine pixel resolution, and a small device footprint..

While star tracker performance is determined by many factors, a star tracker with finer pixel resolution and a larger aperture will tend to outperform a device with coarser resolution and a smaller aperture. Pixel resolution and aperture area cannot be set arbitrarily—to see a sufficient number of stars at all attitudes, a minimum field of view is required for a given aperture area and sensor pixel count. The red, green, and blue curves capture this lower bound for three sensor sizes, a 50 ms exposure, and an assumed requirement of 1000 photons for adequate star detection. Star tracker data points are colored by the most appropriate lower-bound curve.

Beyond offering high image quality with a small mass/volume, folded optics offer advantages in radiation shielding and stray light rejection. As shown in Figure 1, the image sensor is not exposed directly to incoming rays, meaning that radiation shielding can be added directly in front of the sensor. High-energy single event upsets are mitigated through software and hardware redundancy and appropriate data processing.

The annular aperture of the folded optic means that relatively compact shielding can be added at the entrance pupil, leading to more efficient baffling than conventional circular apertures can offer. Further, baffles are constructed internally within the optic. As a result, the influence of stray light is greatly reduced.

UST Design: Lens design was performed with the aid of the optical ray tracing software package Zemax (Zemax LLC, Redmond, WA). Zemax is a powerful and widely used tool that is specifically designed to enable design and modeling of imaging optics. Figure 3 shows images of the optical design, rendered by Zemax. The 90 mm focal length is folded into a less than 30 mm depth using multiple mirrored surfaces, each with optical focusing power. The aperture diameter is 90 mm (giving a traditional f-number of 1.0), with an annulus width of 5 mm. Despite the obscuration in the center of the annulus, the resulting aperture area is comparable to that achieved with much larger and heavier existing star trackers.

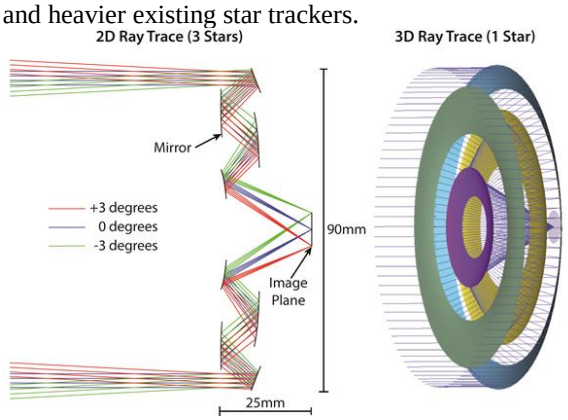

Figure 3: Illustration of Optical Ray Paths Through the Folded Optic Lens. For clarity, only the reflective lens surfaces are shown and the supporting substrate is hidden. The two-dimensional plot on the left shows rays incident from three stars (distinguished by color) and how each set of rays is focused onto the detector plane. The three-dimensional plot on the right shows the same information for a single star, but illustrates the annular nature of the lens.

To fully exploit the high pixel resolution of the image sensor, it is necessary for the lens to also achieve a high optical resolution. Optical resolution is often characterized by examining the lens point spread function (PSF) across the field of view of the imager. The PSF describes the signal resulting from imaging a point-like source such as a star. If the PSF is on the same scale as the pixel pitch, then a sharp image will be read by the sensor. However, if the PSF extends across many pixels, the image will appear blurry and full sensor resolution is not achieved. Poor quality

lenses will often exhibit broad, irregular PSFs and/or PSFs that deteriorate toward the edges of the image. Interestingly, a small amount of defocus is often employed in star trackers to broaden the PSF for centroiding purposes. However, even in this case, there are strict requirements on the PSF, as it should broaden uniformly across the image in order to give consistent image characteristics. Figure 4 shows point spread functions for our folded optic lens, as calculated by Zemax.

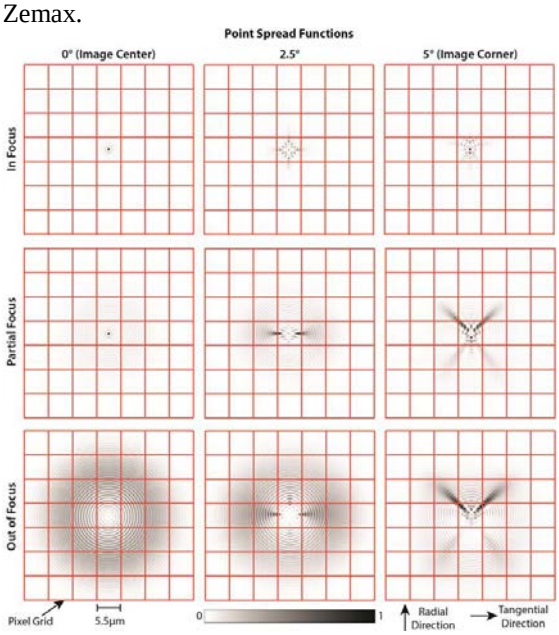

Figure 4: Point Spread Functions for the Folded Optic Lens Design. Each column represents a different location in the image: the left column is in the center of the image sensor, where the tightest PSFs are typically found; the center column is for a star at 2.5°; while the right column is for a 5° star, which is at the very corner of our field of view. The rows illustrate varying degrees of defocus. At focus, the PSFs are all on the scale of one pixel, and so result in an image resolution limited by the pixel size. As defocus is introduced, the scale of the PSFs increases consistently across each row, indicating that deliberate defocus can be used with confidence. Note that the partial-focus, zero-degree image has a faint series of lobes in the image, but when this energy is integrated over each pixel, the PSF does broaden significantly.

UST Protoype and Data: Since the optic construction was funded under a different program, basic lens design was taken from the star tracker application, but a more general purpose lens was constructed. For example, mass reduction was not a primary consideration, and the lens was built with a focus adjustment mechanism that would not be required for a star tracker lens. Despite these differences, the manufactured lens exhibited much of the behavior we wanted to test and allowed us to build a brassboard demonstrator. Figure 5 shows the lens mounted to an industrial camera. Lens manufacturing involved precision diamond turning to match the designed surface profiles to within small fractions of a wavelength.

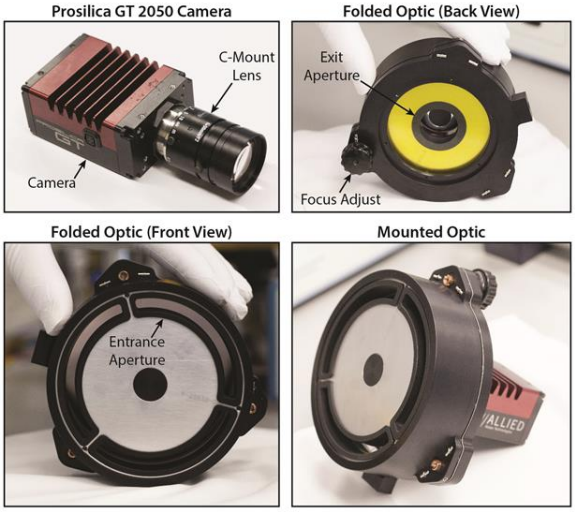

Figure 5: Assembly of the Brassboard UST Prototype. By removing the C-mount lens shown and the camera's front mounting plate, the folded optic lens (upper right and bottom left) can be attached with the focal plane falling on the camera image sensor. The resulting brassboard prototype (lower right) exhibits optical performance similar to the UST design.

Testing was performed by terrestrial night-sky imaging. The hardware described above was used to capture images of stars in the night sky. Basic centroiding and star identification and attitude determination algorithms were tested (off-line) to demonstrate feasibility and estimate performance with real data. This testing provided a validation of the hardware design, the system modeling and analysis, and the projected performance metrics. Below we describe star tracker calibration which, in addition to providing a mathematical model of the imaging system, validates centroiding and star identification methods and provided a self consistency check.

Generally, a calibration target can be any object of known dimensions. In this case, we opted to use the night sky as a calibration target as interstellar angles are very precisely known and the lens would not need to be refocused after calibration (potentially invalidating the calibration). Several calibration images were taken over different camera attitudes, the stars were automatically identified, and an optimization process was used to determine the camera attitudes (one per image) and model parameters that best explained the

data. The resulting model parameters represent the system calibration, as they can be used to model the imaging process. Figure 6 shows an annotated image from a set of calibration data. In this example, nine calibration images were collected of stars in or near the Orion constellation. Across the nine images, 73 usable stars were detected and used to find the nine camera attitudes (27 free parameters) and the camera model (9 free parameters).

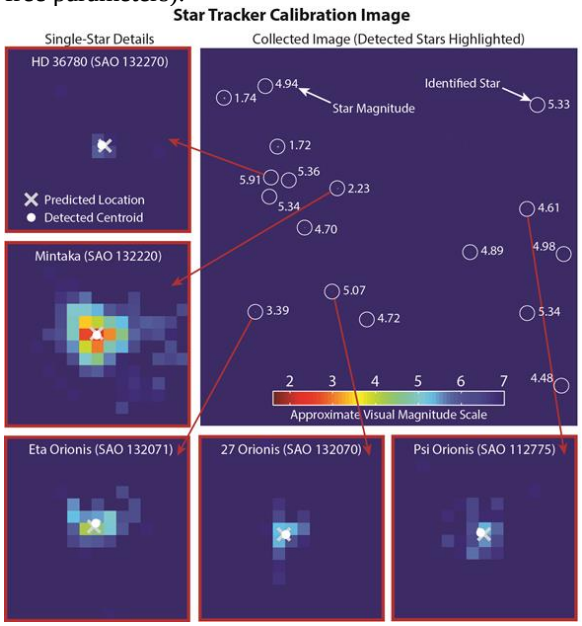

Figure 6: Annotated Calibration Image, With Detail Plots, Illustrating the Identified Stars and Good Agreement Between Detected Star Centroids and the Expected Star Locations. The image shown was collected with a 40 ms exposure and is displayed on a logarithmic scale that approximates the stellar apparent magnitude. The stars that were automatically identified in the image are highlighted with white circles and labeled with their magnitudes. Note that the stars may be difficult to see in the full image due to the high pixel resolution and small star images. The detected centroid locations illustrated are calculated directly from the data, while the predicted locations are generated using the calibrated camera model, the estimated camera attitude, and a star catalog describing the star's physical locations. The agreement between the centroids and the predicted locations is 0.25 pixels RMS, corresponding to approximately 3 arc seconds of variation.

The calibration procedure allowed us to compare the observed star locations in the image (calculated by centroiding) and the predicted locations, as determined by the calibrated camera model. This comparison gives a measure of calibration self-consistency which, in this example, is on the order of 0.25 pixels or 3 arc seconds. The centroiding approach applied is very simple at this stage, and with further work, we believe we should do better than a quarter pixel. However, the level of precision indicated for a single star (3 arc seconds) is still relatively high in an absolute sense, and it should be noted that attitude estimation involves combining estimates from several stars to give a higher precision still.

Conclusions: Creare and our team members have designed, developed, and tested an ultra compact star tracker specifically intended for small satellites. Our design is based on proprietary "folded optics" technology previously developed by partner for use in military and commercial optical applications that require a compact footprint and high performance. Furthermore, the design utilizes recent advances in high pixel count CMOS imaging sensor technology. The folded optics design is superior to conventional refractive optics in miniature star trackers because: (1) the compact footprint is achieved without sacrificing accuracy; (2) the light-gathering aperture is much greater, leading to better sensitivity; (3) the aperture geometry makes the shielding baffles smaller; and (4) the imaging sensor can be shielded efficiently from cosmic radiation. During our feasibility demonstration project, we demonstrated a pointing accuracy of the order of 1 arc second testing a brassboard model of our design. We furthermore completed the design, performed analysis to determine the optimal design parameters, and confirmed the brassboard sensitivity and resolution.